

Protecting entanglement in superconducting qubits

Jing Zhang,^{1,2,*} Yu-xi Liu,^{1,3} Chun-Wen Li,² Tzyh-Jong Tarn,⁴ and Franco Nori^{1,3,5}

¹*Advanced Science Institute, The Institute of Physical and Chemical Research (RIKEN), Wako-shi, Saitama 351-0198, Japan*

²*Department of Automation, Tsinghua University, Beijing 100084, P. R. China*

³*CREST, Japan Science and Technology Agency (JST), Kawaguchi, Saitama 332-0012, Japan*

⁴*Department of Electrical and Systems Engineering,
Washington University, St. Louis, MO 63130, USA*

⁵*Center for Theoretical Physics, Physics Department, Center for the Study of Complex Systems,
The University of Michigan, Ann Arbor, Michigan 48109-1040, USA*

(Dated: November 4, 2018)

When a two-qubit system is initially maximally-entangled, two independent decoherence channels, one per qubit, would greatly reduce the entanglement of the two-qubit system when it reaches its stationary state. We propose a method on how to minimize such a loss of entanglement in open quantum systems. We find that the quantum entanglement of general two-qubit systems with controllable parameters can be protected by tuning both the single-qubit parameters and the two-qubit coupling strengths. Indeed, the maximum fidelity F_{\max} between the stationary entangled state, ρ_{∞} , and the maximally-entangled state, ρ_m , can be about $2/3 \approx \max\{\text{tr}(\rho_{\infty}\rho_m)\} = F_{\max}$, corresponding to a maximum stationary concurrence, C_{\max} , of about $1/3 \approx C(\rho_{\infty}) = C_{\max}$. This is significant because the quantum entanglement of the two-qubit system can be protected, even for a long time. We apply our proposal to several types of two-qubit superconducting circuits, and show how the entanglement of these two-qubit circuits can be optimized by varying experimentally-controllable parameters.

PACS numbers: 85.25.-j, 03.67.Lx, 03.67.Mn

I. INTRODUCTION

Quantum information processing using superconducting qubits (see, e.g., [1, 2, 3, 4]) has made remarkable advances in the past few years. One-qubit and two-qubit quantum circuits (see, e.g., [5, 6, 7, 8, 9, 10, 11]) have been realized experimentally in superconducting systems. One of the most important issues in quantum information processing is how to couple two qubits, which has been widely studied theoretically and experimentally in superconducting quantum circuits (see, e.g., [5, 6, 7, 8, 9, 10, 11, 12, 13, 14, 15, 16, 17, 18, 19, 20, 21, 22, 23, 24, 25]). To couple two qubits, there are two types of approaches: (1) direct coupling and (2) indirect coupling. Examples of qubit-qubit direct coupling include, e.g., capacitively-coupled charge qubits [5, 6] or inductively-coupled flux qubits [8, 9, 12]. Examples of indirect coupling include, e.g., qubit-qubit coupling via a quantum LC oscillator or an inductance [15, 16], a Josephson junction or an extra superconducting qubit acting as a coupler [18, 19], a nanomechanical oscillator [20], or a one or three-dimensional transmission line resonator [21, 22, 23]. The main merit of indirect coupling is that any two qubits can be selectively coupled in a controllable way (see, e.g., [24]). By tuning some control parameters, one can continuously adjust the coupling strengths between qubits, which can be further used to switch between one-qubit and two-qubit operations.

Although maximally-entangled states can be prepared either by directly- or by indirectly-coupled two-qubit superconducting quantum circuits [25], another equivalently important issue is to *protect* these entangled states in an open environment. Some entanglement-protection strategies have been proposed. For instance, it has been recognized [26, 27] that a *common* dissipative environment, e.g., a heat bath, would be helpful to protect the entanglement of two-qubit systems. Specifically, a common dissipative environment would lead to a collective decoherence channel which may induce a so-called decoherence-free subspace [28] to protect special two-qubit entangled states.

Even though a single collective decoherence channel could be used, in principle, to protect two-qubit entangled states, it is very difficult to obtain such a channel in experimental solid-state systems (e.g., superconducting quantum circuits). *Independent* decoherence channels usually lead to disentanglement [29]. This loss of entanglement cannot be recovered by local operations and classical communications, when the two qubits reach their stationary states. Even worse, a mixture of the “independent decoherence” and the “collective decoherence” channels may destroy the decoherence-free subspace and lead to a failure of the entanglement protection. Thus, it is very challenging to protect entanglement in the presence of such a dissipative environment, with independent decoherence channels acting on each qubit.

In this work, we propose a two-qubit entanglement-protection strategy. We find that quantum entanglement can be partially protected even when the two qubits interact *independently* with their own separate environments. Our proposed strategy requires that both the single-

*Electronic address: jing-zhang@mail.tsinghua.edu.cn

qubit oscillating frequencies and the coupling strengths between qubits should be tunable. Therefore, our proposal could be applied to several typical superconducting quantum circuits, and other tunable solid-state qubit systems.

This paper is organized as follows: in Sec. II we present our main results for general two-qubit systems. The entanglement protection for directly- and indirectly-coupled superconducting qubits via an inductive or a capacitive coupler is presented in Sec. III and Sec. IV. In Sec. V, we study the entanglement protection in superconducting qubit circuits interacting with controllable squeezed modes in cavities or resonators (e.g., circuit QED). Conclusions and discussions are given in Sec. VI.

II. GENERAL RESULTS

We consider two coupled qubits with a general Hamiltonian

$$H_A = \mu_1 \left[\exp(-i\theta_1) \sigma_+^{(1)} \sigma_+^{(2)} + \exp(i\theta_1) \sigma_-^{(1)} \sigma_-^{(2)} \right] + \mu_2 \left[\exp(-i\theta_2) \sigma_+^{(1)} \sigma_-^{(2)} + \exp(i\theta_2) \sigma_-^{(1)} \sigma_+^{(2)} \right] + \sum_{j=1}^2 \frac{\omega_{aj}}{2} \sigma_z^{(j)}, \quad (1)$$

where the Planck constant \hbar is assumed to be 1. Here, $\sigma_{\pm}^{(j)} = \sigma_x^{(j)} \pm i\sigma_y^{(j)}$, and $\sigma_x^{(j)}$, $\sigma_y^{(j)}$, $\sigma_z^{(j)}$ are the ladder and Pauli operators of the j -th qubit. The frequency of the j -th qubit is denoted by ω_{aj} . The real coefficients μ_1 (with phase θ_1) and μ_2 (with phase θ_2) correspond to the $\sigma_-^{(1)} \sigma_-^{(2)}$ and $\sigma_-^{(1)} \sigma_+^{(2)}$ coupling strengths, which are assumed to be tunable parameters.

The qubits also interact with uncontrollable degrees of freedom in the environment. If the two qubits interact independently with their own environments, then, under the Born-Markov approximation [30], we can obtain the following master equation:

$$\dot{\rho} = -i[H_A, \rho] + \sum_{j=1}^2 \Gamma_1 \mathcal{D}[\sigma_-^{(j)}] \rho + \sum_{j=1}^2 2\Gamma_{\phi} \mathcal{D}[\sigma_z^{(j)}] \rho, \quad (2)$$

where the super-operator $\mathcal{D}[L]\rho$ is defined as:

$$\mathcal{D}[L]\rho = L\rho L^\dagger - \frac{1}{2}L^\dagger L\rho - \frac{1}{2}\rho L^\dagger L,$$

and Γ_1 , Γ_{ϕ} represent the relaxation and pure dephasing rates for each qubit, respectively. In order to simplify our discussions, it is assumed that the two qubits have the same relaxation and pure dephasing rates.

Below, we will use the concurrence $C(\rho)$:

$$C(\rho) = \max\{\lambda_1 - \lambda_2 - \lambda_3 - \lambda_4, 0\}, \quad (3)$$

to quantify the quantum entanglement between the two qubits (see Ref. [31]), where the λ_i 's are the square roots

of the eigenvalues, in decreasing order, of the matrix

$$M = \rho(\sigma_y^{(1)} \sigma_y^{(2)}) \rho^* (\sigma_y^{(1)} \sigma_y^{(2)}),$$

and ρ^* is the complex conjugate of the density matrix ρ .

If the two qubits do not interact with each other, i.e., $\mu_1 = \mu_2 = 0$ in Eq. (2), the stationary state of the two qubits should be the ground state $\rho_{\infty}^u = |00\rangle\langle 00|$ (see, e.g., [29]), where the superscript “ u ” refers to “uncontrolled” qubit system. Since $\rho_{\infty}^u = |00\rangle\langle 00|$ is a separable state, the entanglement between two qubits is completely *lost* even if they are initially prepared in a maximally-entangled state. However, the following discussions show that *the entanglement can be partially protected by tuning the interaction strength μ_1 and the single-qubit frequencies ω_{aj} in Eq. (1).*

A. Strong interaction regime: $\mu_i \sim 10^{-1}(\omega_{a1} + \omega_{a2})$

Let us now study the regime where the coupling strengths μ_1 and μ_2 are about one-order of magnitude smaller than the sum of the two single-qubit frequencies: $\Omega = \omega_{a1} + \omega_{a2}$, and the phases θ_1 , θ_2 are both time-independent parameters. For such systems, we have the following results:

The solution $\rho(t)$ of Eq. (2) tends to a stationary state

$$\rho_{\infty} = p\rho_m + (1-p)\rho_s \quad (4)$$

as a convex combination of a maximally-entangled state ρ_m :

$$\begin{aligned} \rho_m &= \frac{1}{2} \left(|00\rangle + e^{i(\theta_1 - \phi)} |11\rangle \right) \left(\langle 00| + e^{-i(\theta_1 - \phi)} \langle 11| \right) \\ &= \frac{1}{2} \begin{pmatrix} 1 & & \exp[-i(\theta_1 - \phi)] & \\ & 0 & & \\ \exp[i(\theta_1 - \phi)] & & 0 & \\ & & & 1 \end{pmatrix} \end{aligned}$$

and a diagonal separable state ρ_s :

$$\rho_s = \begin{pmatrix} 1 - 3\beta & & & \\ & \beta & & \\ & & \beta & \\ & & & \beta \end{pmatrix},$$

where

$$\beta = \frac{1}{8} \left(1 - \sqrt{1 - \frac{8\Gamma_2}{\Gamma_1} p^2} \right).$$

The subscript “ m ” is an abbreviation of “maximally-entangled”, and the subscript “ s ” refers to “separable”. $|0\rangle$, $|1\rangle$ are the two eigenstates of a single qubit. The parameters p , ϕ can be expressed as:

$$\begin{aligned} p &= \frac{\sqrt{\Omega^2 + 64\Gamma_2^2}/8\mu_1}{2\Gamma_2/\Gamma_1 + (\Omega^2 + 64\Gamma_2^2)/64\mu_1^2}, \\ \phi &= \arctan \left(-\frac{8\Gamma_2}{\Omega} \right). \end{aligned} \quad (5)$$

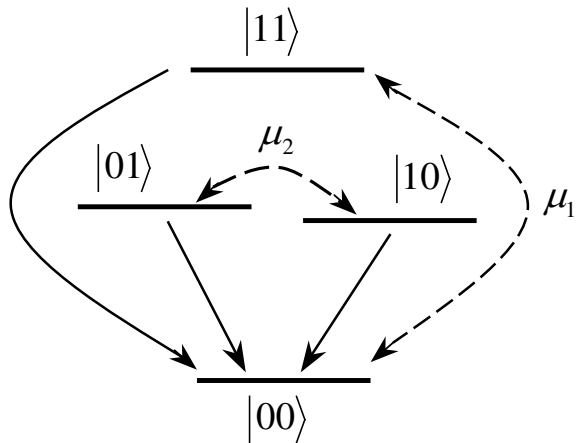


FIG. 1: Schematic diagram of the energy transitions between the four eigen-states: $|00\rangle$, $|11\rangle$, $|10\rangle$, and $|01\rangle$. The solid arrows denote the decays caused by independent relaxation and dephasing channels. The dashed arrows represent the coherent superpositions caused by the interactions between qubits (with interaction strengths μ_1 and μ_2 , respectively).

Γ_2 in Eq. (5) is the dephasing rate that is defined as: $\Gamma_2 = \Gamma_1/2 + \Gamma_\phi$.

The concurrence C of the stationary state ρ_∞ (hereafter called the stationary concurrence) and the fidelity F between ρ_∞ and the maximally-entangled state ρ_m (hereafter called the stationary fidelity) are given by:

$$C(\rho_\infty) = \max \left\{ \frac{8\mu_1\sqrt{\Omega^2 + 64\Gamma_2^2} - 64\mu_1^2\Gamma_2/\Gamma_1}{128\mu_1^2\Gamma_2/\Gamma_1 + (\Omega^2 + 64\Gamma_2^2)}, 0 \right\},$$

$$F(\rho_\infty) = \text{tr}(\rho_m\rho_\infty) = \frac{4\mu_1\sqrt{\Omega^2 + 64\Gamma_2^2} - 32\mu_1^2\Gamma_2/\Gamma_1}{128\mu_1^2\Gamma_2/\Gamma_1 + (\Omega^2 + 64\Gamma_2^2)} + \frac{1}{2}. \quad (6)$$

The derivation of Eq. (6) is given in Appendix A.

Our calculations show that the stationary concurrence $C(\rho_\infty)$ and fidelity $F(\rho_\infty)$ are not affected by the interaction strength μ_2 . Indeed, μ_2 induces a coherent superposition of the two eigen-states $|01\rangle$ and $|10\rangle$ (see Fig. 1). These two states always decay to the two-qubit ground state $|00\rangle$, when subject to independent relaxation and dephasing channels. Thus, μ_2 does not affect the stationary state ρ_∞ . However, the interaction strength μ_1 induces a coherent superposition of the two eigen-states $|00\rangle$ and $|11\rangle$. Of course, $|00\rangle$ is already in the ground state, while the state $|11\rangle$ can be partially recovered from $|00\rangle$ by the coherent superposition caused by μ_1 . Therefore, the stationary concurrence $C(\rho_\infty)$ and fidelity $F(\rho_\infty)$ only depend on μ_1 .

Equation (6) shows that the maximum concurrence

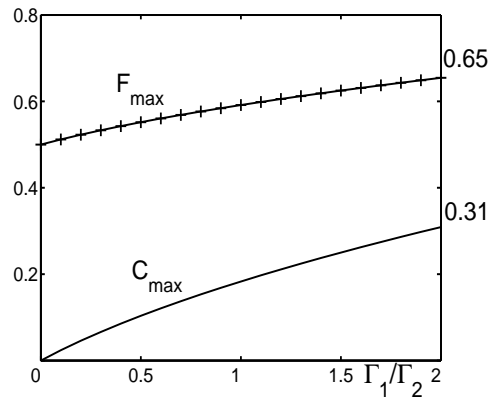


FIG. 2: Maximum concurrence C_{\max} and maximum fidelity F_{\max} , versus the ratio Γ_1/Γ_2 of the relaxation rates, as given in Eq. (7). Note that $C_{\max} \rightarrow 0.31$ and $F_{\max} \rightarrow 0.65$ when $\Gamma_1/\Gamma_2 \rightarrow 2$.

C_{\max} and the maximum fidelity F_{\max} , where

$$C_{\max} = \frac{1}{4} \left(\sqrt{\frac{2\Gamma_1}{\Gamma_2} + 1} - 1 \right),$$

$$F_{\max} = \frac{1}{8} \left(\sqrt{\frac{2\Gamma_1}{\Gamma_2} + 1} - 1 \right) + \frac{1}{2}, \quad (7)$$

can be obtained when the parameters μ_1 and Ω satisfy

$$\mu_1 = \frac{\Gamma_1}{8} \times \frac{\sqrt{\Omega^2 + 64\Gamma_2^2}}{\sqrt{2\Gamma_1\Gamma_2 + \Gamma_2^2 + \Gamma_2}}. \quad (8)$$

The maximum concurrence C_{\max} and fidelity F_{\max} , given in Eq. (7), are plotted in Fig. 2. This clearly shows that the concurrence C_{\max} and fidelity F_{\max} in Eq. (7) increase when the ratio

$$\frac{\Gamma_1}{\Gamma_2} = \frac{\Gamma_1}{\Gamma_1/2 + \Gamma_\phi} \quad (9)$$

increases, and the highest concurrence and fidelity

$$C_{\max} \rightarrow \frac{\sqrt{5} - 1}{4} \approx 0.31, \quad (10)$$

$$F_{\max} \rightarrow \frac{\sqrt{5} + 3}{8} \approx 0.65 \quad (11)$$

can be obtained when $\Gamma_2 \rightarrow \Gamma_1/2$, i.e., $\Gamma_\phi \rightarrow 0$.

The obtained maximum concurrence C_{\max} may not be high enough to be used for demanding tasks in quantum information processing. However, there are two possible ways to increase the stationary entanglement. First, the ratio Γ_1/Γ_2 in Eq. (9) can approach the optimal value 2 for certain systems. For example, if the superconducting charge or flux qubits are at their degenerate points [1, 2, 3], the optimal value 2 might be obtained. In this case, the optimal concurrence and fidelity can be obtained, as shown in Eqs. (10) and (11).

Second, Eq. (7) shows that the maximum fidelity F_{\max} between the stationary state ρ_∞ and the maximally-entangled state ρ_m is always larger than 0.5, which makes it possible to introduce additional entanglement purification process to increase the proportion of the maximally-entangled state ρ_m . Even if the concurrence and fidelity reach the optimal values, as in Eqs. (10) and (11), we can, in principle, further increase the stationary entanglement by using purification strategies, e.g., as in Refs. [32, 33].

B. Weak interaction regime: $\mu_i \ll 10^{-1}(\omega_{a1} + \omega_{a2})$

The results obtained in subsection II A cannot be efficiently applied to the case when $\mu_1, \mu_2 \ll 10^{-1}\Omega$ (e.g., when μ_1, μ_2 are two orders of magnitude smaller than Ω). In fact, the optimal condition (8) shows that we can obtain the maximum concurrence C_{\max} and fidelity F_{\max} only when

$$\mu_1 = \frac{\Gamma_1}{8} \times \frac{\sqrt{\Omega^2 + 64\Gamma_2^2}}{\sqrt{2\Gamma_1\Gamma_2 + \Gamma_2^2} + \Gamma_2} \geq \frac{\Gamma_1}{8(\sqrt{5} + 1)\Gamma_2} \Omega.$$

Thus, if $\mu_1 \ll 10^{-1}\Omega$, then, optimally, the ratio Γ_1/Γ_2 should be very small. In this case, from Eq. (6), the obtained maximum stationary concurrence C_{\max} will be extremely small. Alternatively, in order to avoid this problem, a time-dependent interaction between qubits should be introduced:

If the phase θ_1 in Eq. (1) could be tuned to be

$$\theta_1 = \Omega t + \phi_0 = (\omega_{a1} + \omega_{a2})t + \phi_0,$$

the obtained long-time state ρ_∞ will be a time-dependent state

$$\rho_\infty(t) = \frac{\mu_1\Gamma_1}{2\mu_1^2 + \Gamma_1\Gamma_2} \tilde{\rho}_m(t) + \left(1 - \frac{\mu_1\Gamma_1}{2\mu_1^2 + \Gamma_1\Gamma_2}\right) \tilde{\rho}_s$$

as a convex combination of a time-dependent maximally-entangled state

$$\tilde{\rho}_m(t) = \frac{1}{2} \begin{pmatrix} 1 & & e^{-i(\Omega t + \phi_0 - \frac{\pi}{2})} \\ & 0 & \\ e^{i(\Omega t + \phi_0 - \frac{\pi}{2})} & & 1 \end{pmatrix}$$

and a time-independent diagonal separable state $\tilde{\rho}_s$:

$$\tilde{\rho}_s = \begin{pmatrix} 1 - 3\tilde{\beta} & & & \\ & \tilde{\beta} & & \\ & & \tilde{\beta} & \\ & & & \tilde{\beta} \end{pmatrix},$$

where

$$\tilde{\beta} = \frac{1}{8} \left(1 - \sqrt{1 - \frac{8\Gamma_2}{\Gamma_1} \left(\frac{\mu_1\Gamma_1}{2\mu_1^2 + \Gamma_1\Gamma_2}\right)^2}\right).$$

The corresponding stationary concurrence and fidelity can now be expressed as:

$$C(\rho_\infty) = \max \left\{ \frac{\mu_1(\Gamma_1 - \mu_1)}{2\mu_1^2 + \Gamma_2\Gamma_1}, 0 \right\},$$

$$F(\rho_\infty) = \frac{\mu_1(\Gamma_1 - \mu_1)}{4\mu_1^2 + 2\Gamma_1\Gamma_2} + \frac{1}{2}. \quad (12)$$

For the same reason discussed in subsection II A, the stationary concurrence $C(\rho_\infty)$ and fidelity $F(\rho_\infty)$ are not affected by the interaction strength μ_2 . The proof of Eq. (12) is similar to the proof of Eq. (6). From Eq. (12), the maximum stationary concurrence and fidelity

$$C_{\max} = \frac{1}{4} \left(\sqrt{\frac{2\Gamma_1}{\Gamma_2} + 1} - 1 \right),$$

$$F_{\max} = \frac{1}{8} \left(\sqrt{\frac{2\Gamma_1}{\Gamma_2} + 1} - 1 \right) + \frac{1}{2} \quad (13)$$

can be obtained when

$$\mu_1 = \frac{\Gamma_1\Gamma_2}{\sqrt{2\Gamma_1\Gamma_2 + \Gamma_2^2} + \Gamma_2}. \quad (14)$$

A higher stationary concurrence and fidelity can be obtained, as in the strong interaction regime, by increasing the ratio Γ_1/Γ_2 .

Below, we apply the above results to several superconducting circuits and discuss how their parameters can be varied so that the stationary concurrence and fidelity can be maxima.

III. DIRECT COUPLING BETWEEN SUPERCONDUCTING QUBITS

A. Two capacitively-coupled charge qubits

Let us first study the superconducting circuit shown in Fig. 3, where two single Cooper pair boxes (CPBs) are connected via a small capacitor [5, 6]. The Hamiltonian of the total system can be

$$H_A = \sum_{j=1}^2 [4E_C(\hat{n}_j - n_{gj})^2 - E_J(\Phi_{xj}) \cos \hat{\phi}_j] + 4J\hat{n}_1\hat{n}_2, \quad (15)$$

where $\hat{\phi}_j$ is a phase operator denoting the phase drop across the j -th CPB; $\hat{n}_j = -i\partial/(\partial\hat{\phi}_j)$, which represents the number of Cooper pairs on the island electrode, is the conjugate operator of $\hat{\phi}_j$. The reduced charge number n_{gj} , in units of the Cooper pairs ($2e$), can be given by $n_{gj} = -C_g V_{gj}/2e$, where the parameters C_g and V_{gj} are the gate capacitance and gate voltage of the j -th CPB. The Josephson energy $E_J(\Phi_{xj})$ of the j -th dc SQUID is

$$E_J(\Phi_{xj}) = 2E_J^0 \cos \left(\pi \frac{\Phi_{xj}}{\Phi_0} \right),$$

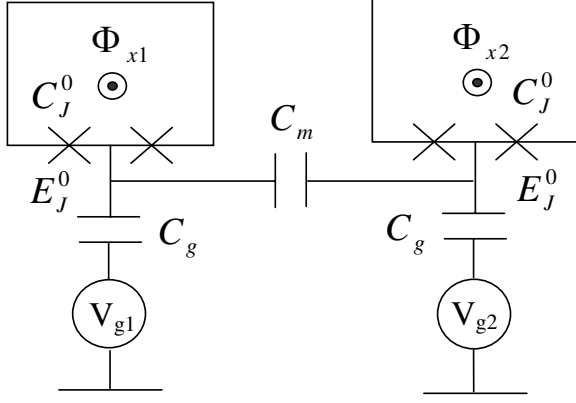


FIG. 3: Schematic diagram of two capacitively coupled CPBs.

where E_J^0 represents the Josephson energy of a single Josephson junction [34]; Φ_{xj} denotes the external flux piercing the SQUID loop of the j -th CPB; and Φ_0 is the flux quantum. The coupling constant J between two CPBs is

$$J = \frac{e^2 C_m}{(C_g + 2C_J^0)^2 - C_m^2},$$

where C_J^0 and C_m are the capacitance of a single Josephson junction and the coupling capacitance between two CPBs. $E_C = e^2/2(C_g + 2C_J^0)$ is the single-electron charging energy of a single CPB. For simplicity, we assume that E_C and E_J^0 are the same for the two CPBs.

Near $n_{gj} = 0.5$, which is called the charge degenerate point, the two energy levels of the j -th CPB corresponding to $n_j = 0, 1$ are close to each other and far separated from other high-energy levels. In this case, a single CPB can be approximately considered as a two-level system. In the charge basis, the Hamiltonian H_A in Eq. (15) can be written as [2]:

$$H_A = \sum_{j=1}^2 \left(-\frac{1}{2} E_C(n_{gj}) \tilde{\sigma}_z^{(j)} - \frac{1}{2} E_J(\Phi_{xj}) \tilde{\sigma}_x^{(j)} \right) + J \tilde{\sigma}_z^{(1)} \tilde{\sigma}_z^{(2)}, \quad (16)$$

where $E_C(n_{gj}) = 4E_C(1 - 2n_{gj})$ and the Pauli operators are defined as:

$$\begin{aligned} \tilde{\sigma}_x^{(j)} &= |0\rangle_{jj}\langle 1| + |1\rangle_{jj}\langle 0|, \\ \tilde{\sigma}_z^{(j)} &= |0\rangle_{jj}\langle 0| - |1\rangle_{jj}\langle 1|. \end{aligned}$$

Here, $|0\rangle_j$ and $|1\rangle_j$ are the charge states with the Cooper pair numbers $n_j = 0, 1$, respectively.

Rewriting Eq. (16) using the eigenstates of the single-qubit Hamiltonian, we have

$$H_A = \sum_{j=1}^2 \frac{\omega_{aj}}{2} \sigma_z^{(j)} + J \prod_{j=1}^2 \left(\frac{E_{Jj}}{\omega_{aj}} \sigma_x^{(j)} - \frac{E_{Cj}}{\omega_{aj}} \sigma_z^{(j)} \right),$$

with $\omega_{aj} = (E_{Cj}^2 + E_{Jj}^2)^{1/2}$, $E_{Cj} = E_C(n_{gj})$, and $E_{Jj} = E_J(\Phi_{xj})$. The new Pauli operators $\sigma_x^{(j)}$ and $\sigma_z^{(j)}$ are defined by the eigenstates $|+\rangle_j$ and $|-\rangle_j$ of the j -th qubit as:

$$\begin{aligned} \sigma_x^{(j)} &= |+\rangle_j \langle -| + |-\rangle_j \langle +|, \\ \sigma_z^{(j)} &= |+\rangle_j \langle +| - |-\rangle_j \langle -|, \end{aligned}$$

where

$$\begin{aligned} |+\rangle_j &= \cos \theta_j |0\rangle_j - \sin \theta_j |1\rangle_j, \\ |-\rangle_j &= \sin \theta_j |0\rangle_j + \cos \theta_j |1\rangle_j. \end{aligned}$$

Here, $\theta_j = [\arctan(-E_{Jj}/E_{Cj})]/2$.

Now, the two-qubit state $\rho(t)$ evolves following the master equation:

$$\dot{\rho} = -i[H_A, \rho] + \sum_{j=1}^2 \Gamma_1 \mathcal{D}[\sigma_-^{(j)}] \rho + \sum_{j=1}^2 2\Gamma_\phi \mathcal{D}[\sigma_z^{(j)}] \rho.$$

Let us now assume that the two qubits are both in the charge degenerate point $n_{gj} = 0.5$ with $E_{Cj} = 0$, so that the dephasing effects can be minimized. In this case, we have $\Gamma_\phi = 0$, which means that $\Gamma_2 = \Gamma_1/2 + \Gamma_\phi = \Gamma_1/2$. Further, from $E_{Cj} = 0$, we have:

$$\begin{aligned} H_A &= \sum_{j=1}^2 \frac{E_J(\Phi_{xj})}{2} \sigma_z^{(j)} + J \sigma_x^{(1)} \sigma_x^{(2)} \\ &= \sum_{j=1}^2 \frac{E_J(\Phi_{xj})}{2} \sigma_z^{(j)} + \frac{J}{4} (\sigma_+^{(1)} \sigma_+^{(2)} + \sigma_-^{(1)} \sigma_-^{(2)}) \\ &\quad + \frac{J}{4} (\sigma_+^{(1)} \sigma_-^{(2)} + \sigma_-^{(1)} \sigma_+^{(2)}). \end{aligned}$$

In some experiments (e.g., [5]), the coupling strength J is of the same order of

$$\Omega = \sum_{j=1}^2 2E_J^0 \cos\left(\pi \frac{\Phi_{xj}}{\Phi_0}\right),$$

where $J \approx 4$ GHz, $E_J^0 \approx 10$ GHz and the decoherence rates [35] Γ_1, Γ_2 are of the order of 10–100 MHz $\ll J, \Omega$.

If we let $\Phi_{x1} = \Phi_{x2} = \Phi_x$ and substitute

$$\Omega = 2E_J(\Phi_x), \quad \mu_1 = \frac{J}{4}$$

into Eq. (8), then, in the limit $\Omega \gg \Gamma_1, \Gamma_2$, the maximum concurrence $C_{\max} \approx 0.31$ and fidelity $F_{\max} \approx 0.65$, as in Eqs. (10) and (11), can be obtained, if only

$$J \approx \frac{4}{\sqrt{5} + 1} E_J^0 \cos\left(\pi \frac{\Phi_x}{\Phi_0}\right),$$

or, equivalently,

$$\cos\left(\pi \frac{\Phi_x}{\Phi_0}\right) \approx \frac{\sqrt{5} + 1}{4} \times \frac{J}{E_J^0}.$$

B. Two inductively-coupled flux qubits

Let us now consider a superconducting circuit, as shown in Fig. 4, where two flux qubits are coupled through their mutual inductance. Here, we modify the design used in the experimental device in Ref. [9]. Namely, the small junction of each three-junction flux qubit is replaced by a dc SQUID, from which we can adjust the tunnelling amplitude between the left and right wells (see Fig. 5) of each single flux qubit.

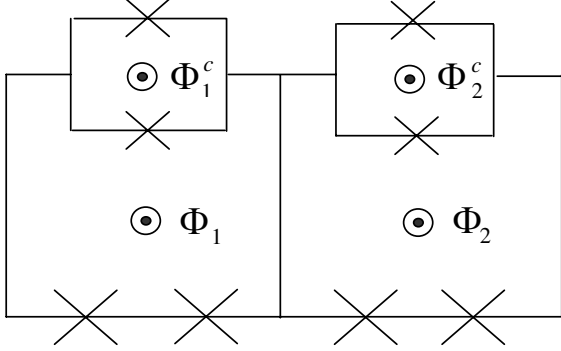


FIG. 4: Schematic diagram of two flux qubits coupled via their mutual inductance.

Near the flux degenerate point $\Phi_j \approx \Phi_0/2$, with the external flux Φ_j piercing the superconducting loop of the j -th qubit, each flux qubit behaves as a two-level system. The total Hamiltonian of the two-qubit system can be expressed as [9]:

$$H_A = -\frac{1}{2} \sum_{j=1}^2 \left[\epsilon(\Phi_j) \tilde{\sigma}_z^{(j)} + \Delta(\Phi_j^c) \tilde{\sigma}_x^{(j)} \right] + J \tilde{\sigma}_z^{(1)} \tilde{\sigma}_z^{(2)}, \quad (17)$$

where

$$\begin{aligned} \tilde{\sigma}_x^{(j)} &= |L_j\rangle\langle R_j| + |R_j\rangle\langle L_j|, \\ \tilde{\sigma}_z^{(j)} &= |L_j\rangle\langle L_j| - |R_j\rangle\langle R_j|, \end{aligned}$$

and $|L_j\rangle, |R_j\rangle$ are the two lowest energy-states in the left and right wells of the j -th flux qubit (see Fig. 5). The parameter $\epsilon(\Phi_j)$ denotes the energy difference between $|L_j\rangle$ and $|R_j\rangle$ which can be expressed as:

$$\epsilon(\Phi_j) = 2I_{pj} \left(\Phi_j - \frac{1}{2}\Phi_0 \right),$$

where I_{pj} is the circulating current in the loop of the j -th qubit. The tunnelling amplitude $\Delta(\Phi_j^c)$ between the two wells is tunable by varying the magnetic flux Φ_j^c piercing the j -th dc-SQUID. In the limit

$$0 < \frac{2\pi L_j I_c(\Phi_j^c)}{\Phi_0} - 1 \ll 1,$$

$\Delta(\Phi_j^c)$ can be approximately expressed as [17]:

$$\Delta(\Phi_j^c) \approx \frac{3\Phi_0^2}{8\pi^2 L_j} \left(1 - \frac{\Phi_0}{2\pi L_j I_c(\Phi_j^c)} \right)^2,$$

where L_j is the self-inductance of the superconducting loop of the j -th flux qubit, and

$$I_c(\Phi_j^c) = 2I_0 \left| \cos \left(\frac{\pi \Phi_j^c}{\Phi_0} \right) \right|$$

is the tunable critical current of the j -th dc-SQUID with I_0 being the maximum critical current. The coupling strength J between the two flux qubits is

$$J = M I_{p1} I_{p2},$$

with the mutual inductance M between the two flux qubits.

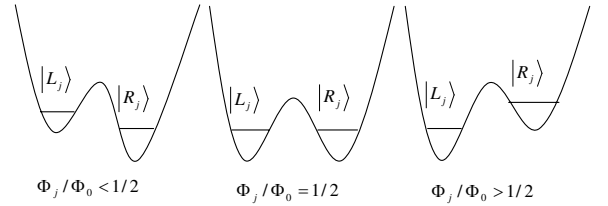


FIG. 5: Schematic diagram of the double-well potential of the j -th flux qubit with the two lowest-energy states for $\Phi_j < \Phi_0/2$, $\Phi_j = \Phi_0/2$, and $\Phi_j > \Phi_0/2$.

Let us now assume that $\Phi_j = \Phi_0/2$, then the two-qubit Hamiltonian in Eq. (17) can be further simplified to

$$\begin{aligned} H_A &= \frac{1}{2} \sum_{j=1}^2 \Delta(\Phi_j^c) \sigma_z^{(j)} + \frac{J}{4} (\sigma_+^{(1)} \sigma_+^{(2)} + \sigma_-^{(1)} \sigma_-^{(2)}) \\ &\quad + \frac{J}{4} (\sigma_+^{(1)} \sigma_-^{(2)} + \sigma_-^{(1)} \sigma_+^{(2)}), \end{aligned}$$

where

$$\begin{aligned} \sigma_x^{(j)} &= |+\rangle_j \langle -| + |-\rangle_j \langle +|, \\ \sigma_z^{(j)} &= |+\rangle_j \langle +| - |-\rangle_j \langle -|, \end{aligned}$$

and

$$\begin{aligned} |+\rangle_j &= \frac{\sqrt{2}}{2} \{ |L_j\rangle - |R_j\rangle \}, \\ |-\rangle_j &= \frac{\sqrt{2}}{2} \{ |L_j\rangle + |R_j\rangle \}. \end{aligned}$$

The decoherence process can be described by the master equation (2) under the Born-Markov approximation. At the degenerate point ($\Phi_j = \Phi_0/2$; $j = 1, 2$), we have $\Gamma_\phi = 0$, which means that $\Gamma_2 = (\Gamma_1/2) + \Gamma_\phi = \Gamma_1/2$.

Let us assume that $\Phi_1^c = \Phi_2^c = \Phi^c$ and substitute

$$\Omega = 2\Delta(\Phi^c), \quad \mu_1 = \frac{J}{4}$$

into Eq. (8), then, in the limit $\Delta(\Phi^c), J \gg \Gamma_1, \Gamma_2$, the maximum concurrence $C_{\max} \approx 0.31$ and fidelity $F_{\max} \approx 0.65$ can be obtained when

$$\Delta(\Phi^c) \approx \frac{\sqrt{5}+1}{2}J.$$

In experiments [9], $\Delta(\Phi^c)$ and J are of the same order (~ 1 GHz) that are far larger than the decoherence rates $\Gamma_1, \Gamma_2 \sim 1\text{--}10$ MHz (see, e.g., [36]). Thus, the above optimal conditions could be realized in experiments.

IV. TUNABLE COUPLING BETWEEN SUPERCONDUCTING QUBITS: STRONG-INTERACTION REGIME

There are two ways to tune the system parameters to achieve the optimal condition (8). One way is by *tuning the sum of the single-qubit oscillating frequencies* Ω , which was used in Sec. III. In this section, we study another way to achieve the optimal condition (8) by *tuning the coupling strength* μ_1 between the two qubits.

A. Variable-coupling between two charge qubits

Many strategies have been proposed to obtain a controllable coupling between qubits (see, e.g., [15, 16, 17, 18, 19, 20, 21, 22, 23, 24]). Let us first study the superconducting circuit shown in Fig. 6, where two CPBs are coupled via an LC oscillator. This strategy was first proposed in Ref. [15] and also investigated by other researchers (e.g., in Ref. [37]). In the charge degenerate point, the two-qubit Hamiltonian in Refs. [1, 15] is

$$H_A = -\sum_{j=1}^2 \frac{1}{2} E_J(\Phi_{xj}) \tilde{\sigma}_x^{(j)} - E_{\text{int}} \tilde{\sigma}_y^{(1)} \tilde{\sigma}_y^{(2)}, \quad (18)$$

with $E_{\text{int}} = E_J(\Phi_{x1})E_J(\Phi_{x2})/E_L$ and $E_J(\Phi_{xj}) = 2E_J^0 \cos(\pi\Phi_{xj}/\Phi_0)$. Here

$$\begin{aligned} \tilde{\sigma}_x^{(j)} &= |0\rangle_j \langle 1| + |1\rangle_j \langle 0|, \\ \tilde{\sigma}_y^{(j)} &= -i|0\rangle_j \langle 1| + i|1\rangle_j \langle 0|, \end{aligned}$$

and $|0\rangle_j, |1\rangle_j$ are the two charge states of the j -th CPB. The quantity E_L in the expression above for the coupling strength E_{int} can be written as:

$$E_L = \left(\frac{2C_J^0}{C_{qb}} \right)^2 \frac{\Phi_0^2}{\pi^2 L},$$

where $C_{qb} = 2C_J^0 C_g [2C_J^0 + C_g]^{-1}$ is the capacitance of a single CPB in the external circuit, and L is the inductance of the coupling current-biased inductor.

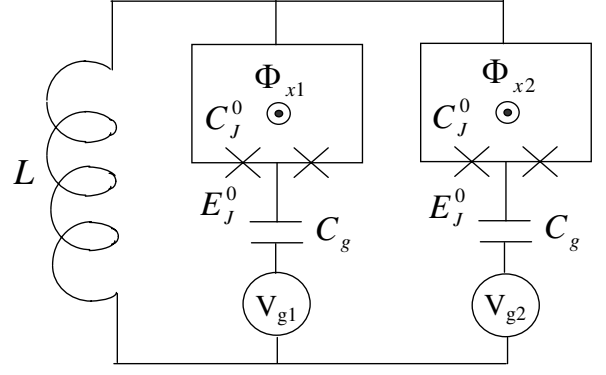


FIG. 6: Schematic diagram of two charge qubits coupled via an LC oscillator.

Rewriting Eq. (18) under the eigenstates of the single-qubit Hamiltonian, we have:

$$\begin{aligned} H_A &= \sum_{j=1}^2 \frac{E_J(\Phi_{xj})}{2} \sigma_z^{(j)} + \frac{E_{\text{int}}}{4} (\sigma_+^{(1)} \sigma_+^{(2)} + \sigma_-^{(1)} \sigma_-^{(2)}) \\ &\quad - \frac{E_{\text{int}}}{4} (\sigma_+^{(1)} \sigma_-^{(2)} + \sigma_-^{(1)} \sigma_+^{(2)}), \end{aligned}$$

where

$$\begin{aligned} \sigma_z^{(j)} &= |+\rangle_j \langle +| - |-\rangle_j \langle -| = -\tilde{\sigma}_x^{(j)}, \\ \sigma_y^{(j)} &= -i|+\rangle_j \langle -| + i|-\rangle_j \langle +| = \tilde{\sigma}_y^{(j)}, \end{aligned}$$

and

$$\begin{aligned} |+\rangle_j &= \frac{1}{\sqrt{2}} \{|0\rangle_j - |1\rangle_j\}, \\ |-\rangle_j &= \frac{1}{\sqrt{2}} \{|0\rangle_j + |1\rangle_j\}. \end{aligned}$$

Now, let $\Phi_{x1} = \Phi_{x2} = \Phi_x$. Since $\Gamma_2 = \Gamma_1/2$ at the charge degenerate point, then, replacing Ω and μ_1 in Eq. (8) by $2E_J(\Phi_x)$ and $E_{\text{int}}/4$, the maximum concurrence $C_{\max} \approx 0.31$ and fidelity $F_{\max} \approx 0.65$ can be obtained when

$$\cos\left(\pi \frac{\Phi_x}{\Phi_0}\right) \approx \frac{1}{\sqrt{5}+1} \times \frac{E_L}{E_J^0},$$

when these conditions hold: $E_L, E_J^0 \gg \Gamma_1, \Gamma_2$.

B. Variable-coupling between two flux qubits

Our strategy can also be applied to flux qubits with controllable coupling. Here, let us consider a superconducting circuit design as in Ref. [18] (see Fig. 7), where two three-junction flux qubits (qubits 1 and 2) are coupled via an auxiliary three-junction flux qubit (qubit 3). This middle flux qubit (qubit 3), acting as a coupler, is connected to qubits 1 and 2 by sharing junctions a and b with the same Josephson energy E_J^0 , while junction c is

smaller than a and b , with Josephson energy αE_J^0 , $\alpha < 1$. By adiabatically eliminating the degrees of freedom of the auxiliary flux qubit 3, the total Hamiltonian of the flux qubits 1 and 2 becomes [18]

$$H_A = -\frac{1}{2} \sum_{j=1}^2 [\epsilon(\Phi_j) \tilde{\sigma}_z^{(j)} + \Delta_j \tilde{\sigma}_x^{(j)}] + J(\Phi_3) \tilde{\sigma}_z^{(1)} \tilde{\sigma}_z^{(2)},$$

where $\epsilon(\Phi_j)$, Δ_j , $j = 1, 2$, $\tilde{\sigma}_z^{(j)}$ and $\tilde{\sigma}_x^{(j)}$ have the same meaning as in subsection III.B. When $\alpha \ll 1$, the coupling strength $J(\Phi_3)$ between the two flux qubits 1 and 2 becomes [18]:

$$J(\Phi_3) \approx \frac{\alpha I_{p1} I_{p2}}{4e^2 E_J^0} \cos\left(2\pi \frac{\Phi_3}{\Phi_0}\right) \equiv J_0 \cos\left(2\pi \frac{\Phi_3}{\Phi_0}\right). \quad (19)$$

From Eq. (19), the coupling strength $J(\Phi_3)$ is tunable by varying the flux Φ_3 piercing the superconducting loop of the auxiliary qubit 3.

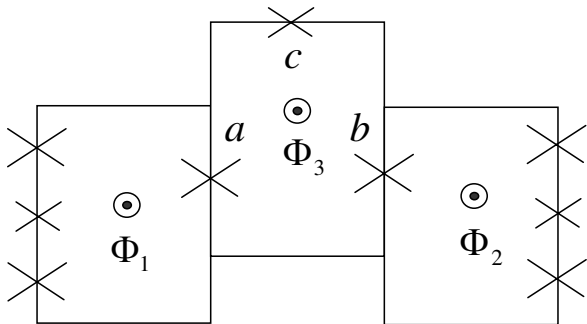


FIG. 7: Schematic diagram of two three-junction flux qubits coupled via an auxiliary flux qubit.

At the flux degenerate point, i.e., $\Phi_j = \Phi_0/2$ for both qubits, and using the eigenstates of the single-qubit Hamiltonian, we have:

$$\begin{aligned} H_A &= \frac{1}{2} \sum_{j=1}^2 \Delta_j \sigma_z^{(j)} + J(\Phi_3) \sigma_x^{(1)} \sigma_x^{(2)} \\ &= \frac{1}{2} \sum_{j=1}^2 \Delta_j \sigma_z^{(j)} + \frac{J(\Phi_3)}{4} (\sigma_+^{(1)} \sigma_+^{(2)} + \sigma_-^{(1)} \sigma_-^{(2)}) \\ &\quad + \frac{J(\Phi_3)}{4} (\sigma_+^{(1)} \sigma_-^{(2)} + \sigma_-^{(1)} \sigma_+^{(2)}). \end{aligned}$$

Since the two flux qubits are at their flux degenerate points, then, replacing Ω and μ_1 in Eq. (8) by $\Delta_1 + \Delta_2$ and $J(\Phi_3)/4$, the maximum stationary concurrence $C_{\max} \approx 0.31$ and fidelity $F_{\max} \approx 0.65$ can be obtained when $J(\Phi_3) \approx (\Delta_1 + \Delta_2)/(\sqrt{5} + 1)$, i.e.,

$$\cos\left(2\pi \frac{\Phi_3}{\Phi_0}\right) \approx \frac{(\Delta_1 + \Delta_2)}{(\sqrt{5} + 1)J_0},$$

when these conditions hold: $\Delta_1, \Delta_2, J_0 \gg \Gamma_1, \Gamma_2$.

From the experiment [18], where Δ_1, Δ_2 and J_0 are of the same order (~ 1 GHz) and far larger than Γ_1, Γ_2 (~ 1 –10 MHz), the above optimal condition could be satisfied by varying the magnetic flux Φ_3 through the middle superconducting loop.

V. TUNABLE COUPLING BETWEEN SUPERCONDUCTING QUBITS: WEAK INTERACTION REGIME

In this section, we study how to protect quantum entanglement in superconducting circuits where two charge qubits are coupled to a one-dimensional transmission line resonator. Since the interaction strength (10–100 MHz) between the two charge qubits coupled via the resonator is far smaller than the single-qubit oscillating frequency (5–15 GHz), then we are now considering the weak-interaction regime. From the analysis in subsection II B, in order to protect entanglement in this case, the following time-dependent interaction Hamiltonian should be introduced:

$$H_{\text{int}} = \mu_1 (e^{-i(\Omega t + \phi_0)} \sigma_+^{(1)} \sigma_+^{(2)} + e^{i(\Omega t + \phi_0)} \sigma_-^{(1)} \sigma_-^{(2)}).$$

The main idea in this section is the following: borrowing strategies that produce controllable squeezed fields in optical cavities (see, e.g., [38]), an auxiliary flux qubit circuit is introduced to squeeze the oscillating mode in the resonator (see Fig. 8). The auxiliary flux qubit circuit in fact acts like a Δ -shaped three-level atom which is further driven by a classical field. By adiabatically eliminating the degrees of freedom of the auxiliary flux qubit circuit, one can obtain a controllable squeezed field in the resonator where the squeezed coefficient is tunable by changing the coupling strength between the classical driving field and the auxiliary flux qubit. With the help of the controllable squeezed field in the resonator, one can continuously adjust the stationary entanglement between the two qubits.

A. Controllable squeezed electric field in a transmission line resonator

We first show how to obtain a controllable squeezed electric field [39, 40, 41, 42] in the resonator by using a theoretical proposal of realizing squeezed states in cavities [38]. The auxiliary flux qubit circuit in our proposal (shown in Fig. 8) acts as a three-level system with Δ -type transition [43, 44].

As depicted in Fig. 9, we are now considering a three-level system with a ground energy level $|g\rangle$, an intermediate energy level $|i\rangle$, and an excited energy level $|e\rangle$. Here, the transitions $|g\rangle \leftrightarrow |i\rangle$ and $|e\rangle \leftrightarrow |i\rangle$ are coupled dispersively to the quantized cavity mode in the resonator, with coupling strengths λ_g and λ_e . The transition $|g\rangle \leftrightarrow |e\rangle$ is coupled dispersively to a classical field with coupling strength λ_d and frequency $\tilde{\Omega}$. In the

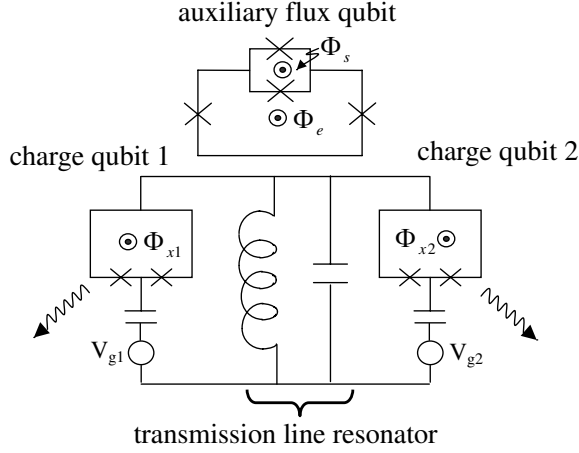


FIG. 8: Schematic diagram of our proposal for protecting quantum entanglement in two charge qubits coupled to a resonator.

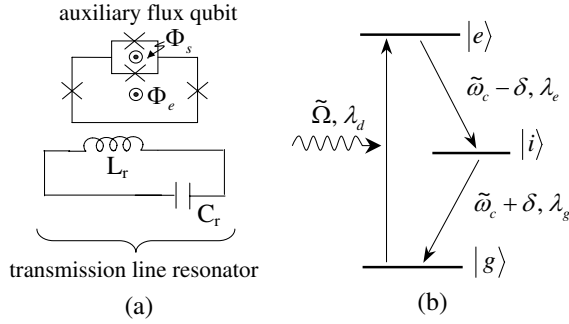


FIG. 9: Schematic diagrams for realizing a controllable squeezed electromagnetic field in a resonator coupled to an auxiliary flux qubit. (a) The auxiliary flux qubit and the transmission line resonator: the parameters in the auxiliary flux qubit are the same as those in Ref. [44]; by varying the flux Φ_s threading through the SQUID loop one can obtain a Δ -shaped three-level artificial atom. (b) Transition energy-level-diagram of the Δ -shaped three-level artificial atom.

rotating-wave approximation, the total Hamiltonian of the three-level artificial atom and the resonator can be expressed as $H = H_0 + V$, with

$$\begin{aligned} H_0 &= \tilde{\omega}_c a^\dagger a - \tilde{\omega}_c |g\rangle\langle g| + \delta |i\rangle\langle i| + \tilde{\omega}_c |e\rangle\langle e|, \\ V &= (\lambda_g a |i\rangle\langle g| + \text{h.c.}) + (\lambda_e a |e\rangle\langle i| + \text{h.c.}) \\ &\quad + (\lambda_d |e\rangle\langle g| e^{-i\Omega t} + \text{h.c.}), \end{aligned} \quad (20)$$

where h.c. means Hermitian conjugate; $\tilde{\omega}_c$ is the frequency of the resonator; δ is defined as a detuning from the energy levels $|e\rangle$ and $|g\rangle$ to the intermediate energy level $|i\rangle$.

Let us initially prepare the artificial atom in the intermediate level $|i\rangle$. With the help of the dispersive-detuning condition:

$$\delta \gg |\lambda_g|, |\lambda_e|, |\tilde{\Omega} - 2\tilde{\omega}_c|,$$

one can obtain the following reduced Hamiltonian by adiabatically eliminating the degrees of freedom of the three-level artificial atom [38]:

$$H_c = \omega_c a^\dagger a + \xi (e^{-i(\tilde{\Omega}t + \tilde{\phi}_0)} a^\dagger{}^2 + e^{i(\tilde{\Omega}t + \tilde{\phi}_0)} a^2), \quad (21)$$

where

$$\omega_c = \tilde{\omega}_c + \frac{2}{\delta} (|\lambda_g|^2 + |\lambda_e|^2)$$

is the effective frequency of the cavity mode; ξ and $\tilde{\phi}_0$ are the effective amplitude and the initial phase of the squeezed field. The relation between ξ and $\tilde{\phi}_0$ is given by

$$\xi \exp(i\tilde{\phi}_0) = \frac{2}{\delta^2} \lambda_d \lambda_g \lambda_e.$$

Notice that one can continuously adjust ξ by varying the coupling strength λ_d between the classical field and the three-level artificial atom.

B. Tunable coupling between qubits

In Fig. 8, let us now consider the interaction between the two charge qubits and the cavity field. After eliminating the degrees of freedom of the auxiliary three-level system, we can obtain the following total Hamiltonian of the charge qubits and the cavity field:

$$\begin{aligned} H &= \xi (e^{-i(\tilde{\Omega}t + \tilde{\phi}_0)} a^\dagger{}^2 + e^{i(\tilde{\Omega}t + \tilde{\phi}_0)} a^2) \\ &\quad + \sum_{j=1}^2 g(\eta_j - \cos \alpha_j \sigma_z^{(j)} + \sin \alpha_j \sigma_x^{(j)}) (a^\dagger + a) \\ &\quad + \frac{1}{2} \sum_{j=1}^2 \omega_{aj} \sigma_z^{(j)} + \omega_c a^\dagger a, \end{aligned} \quad (22)$$

where

$$\omega_{aj} = \sqrt{E_J^2(\Phi_{xj}) + E_C^2(n_{gj})}$$

has the same meaning with the corresponding quantity in Sec. III and IV; $g = -e(C_g/C_\Sigma)V_{\text{rms}}^0$ is the coupling strength between the resonator and a single qubit; C_Σ is the total capacitance of a qubit; $V_{\text{rms}}^0 = \sqrt{\omega_c/2C_r}$ is the root mean square (rms) of the voltage across the LC circuit; C_r is the capacitance of the resonator; $\eta_j = 1 - 2n_{gj}$; and the angle $\alpha_j = \arctan[E_J(\Phi_{xj})/E_C(1 - 2n_{gj})]$.

By using the rotating-wave approximation and assuming that $n_{gj} = 1/2$ ($j = 1, 2$), the total Hamiltonian H in Eq. (22) can be rewritten as [30]:

$$\begin{aligned} H_{JC} &= \omega_c a^\dagger a + \sum_{j=1}^2 \frac{E_J(\Phi_{xj})}{2} \sigma_z^{(j)} + \sum_{j=1}^2 g(a^\dagger \sigma_-^{(j)} + a \sigma_+^{(j)}), \\ &\quad + \xi (e^{-i(\tilde{\Omega}t + \tilde{\phi}_0)} a^\dagger{}^2 + e^{i(\tilde{\Omega}t + \tilde{\phi}_0)} a^2). \end{aligned}$$

Here, to simplify our discussions, we have set $\Phi_{x1} = \Phi_{x2} = \Phi_x$.

We now assume that the qubits and the cavity field are in the dispersive regime, i.e.,

$$\Delta = [E_J(\Phi_x) - \omega_c] \sim 100 \text{ MHz} \gg |g| \sim 10 \text{ MHz}.$$

Thus, we can introduce the following unitary transformation to diagonalize the Hamiltonian H_{JC} :

$$U = \exp \left[\frac{g}{\Delta} \sum_{j=1}^2 (a\sigma_+^{(j)} - a^\dagger\sigma_-^{(j)}) \right].$$

Up to first order in g/Δ , we have

$$\begin{aligned} UH_{JC}U^\dagger &\approx \omega_c a^\dagger a + \xi e^{-i(\tilde{\Omega}t + \tilde{\phi}_0)} a^{\dagger 2} + \xi e^{i(\tilde{\Omega}t + \tilde{\phi}_0)} a^2 \\ &+ \sum_{j=1}^2 \left[\frac{\tilde{\omega}_a}{2} + \frac{4g^2}{\Delta^2} (\xi e^{-i(\tilde{\Omega}t + \tilde{\phi}_0)} a^{\dagger 2} + \text{h.c.}) + \frac{4g^2}{\Delta} a^\dagger a \right] \sigma_z^{(j)} \\ &+ \sum_{j=1}^2 \left[\left(\frac{2g\xi e^{-i(\tilde{\Omega}t + \tilde{\phi}_0)}}{\Delta} a^\dagger + \frac{g^2 \xi e^{-i(\tilde{\Omega}t + \tilde{\phi}_0)}}{\Delta^2} \right) \sigma_+^{(j)} + \text{h.c.} \right] \\ &+ \mu_1 (e^{-i(\tilde{\Omega}t + \tilde{\phi}_0)} \sigma_+^{(1)} \sigma_+^{(2)} + e^{i(\tilde{\Omega}t + \tilde{\phi}_0)} \sigma_-^{(1)} \sigma_-^{(2)}) \\ &+ \mu_2 (\sigma_+^{(1)} \sigma_-^{(2)} + \sigma_-^{(1)} \sigma_+^{(2)}), \end{aligned}$$

where

$$\begin{aligned} \tilde{\omega}_a &= E_J(\Phi_x) + 4g^2/\Delta, \\ \mu_1 &= 2g^2\xi/\Delta^2, \quad \mu_2 = g^2/\Delta. \end{aligned}$$

By adiabatically eliminating the degrees of freedom of the resonator, the following two-qubit Hamiltonian can be obtained:

$$\begin{aligned} H_A &\approx \sum_{j=1}^2 \frac{E_J(\Phi_x)}{2} \sigma_z^{(j)} + \mu_2 (\sigma_+^{(1)} \sigma_-^{(2)} + \sigma_-^{(1)} \sigma_+^{(2)}) \\ &+ \mu_1 (e^{-i(\tilde{\Omega}t + \tilde{\phi}_0)} \sigma_+^{(1)} \sigma_+^{(2)} + e^{i(\tilde{\Omega}t + \tilde{\phi}_0)} \sigma_-^{(1)} \sigma_-^{(2)}). \end{aligned}$$

Here, we have omitted all the single-qubit terms induced by the interaction between qubits and the resonator because of the conditions:

$$E_J(\Phi_x)/2 \gg g^2/\Delta, \quad \xi g/\Delta.$$

As analyzed in subsection A of section V, we can continuously adjust the parameter ξ , thus the coupling strength μ_1 is continuously tunable.

Since the two superconducting charge qubits also interact with the uncontrollable degrees of freedom in the environment (e.g., quantum noises induced by charge fluctuations on the electric gates), the discussed two-qubit system should be considered as an open quantum system. For this two-qubit system, the master equation (2) can be obtained under the Born-Markov approximation [23].

From Eq. (14), at the charge degenerate points for both qubits, we know that the optimal concurrence $C_{\max} \approx 0.31$ and fidelity $F_{\max} \approx 0.65$ can be obtained when

$$\tilde{\Omega} = 2E_J(\Phi_x), \quad \xi = \frac{1}{\sqrt{5}+1} \times \frac{\Delta^2}{g^2} \Gamma_1.$$

Using now the same experimental parameters from Ref. [23]:

$$\begin{aligned} \Delta &= E_J - \omega_r = 5 \text{ GHz} - 4.8 \text{ GHz} = 200 \text{ MHz}, \\ g &= 20 \text{ MHz}, \quad \Gamma_1/2\pi \sim 0.1 \text{ MHz}, \\ \lambda_g, \lambda_e &\sim 10 \text{ MHz}, \quad \delta \sim 100 \text{ MHz}, \end{aligned}$$

the squeezed amplitude ξ is of the order of 1 MHz, which can be realized by a strong microwave driving field with coupling strength $\lambda_d \sim 100$ MHz. These parameters show that our entanglement-protection proposal is experimentally realizable.

Although this section mainly concentrates on how to protect entanglement in two charge qubits coupled to a transmission line resonator, our proposal is also extendable to two flux qubits in a coplanar transmission line resonator [45]. Since the system parameters [45] are almost of the same order of those for charge qubits, there is no essential difference between them, as far as applying our proposal.

VI. CONCLUSIONS

In summary, we propose a strategy to protect quantum entanglement against independent quantum noises in several types of superconducting circuits. For two superconducting qubits coupled strongly via an inductive or a capacitive element, one can tune the stationary entanglement by varying the single-qubit oscillating frequencies or the coupling strengths between the qubits. For superconducting qubits weakly coupled via a quantum cavity (e.g., a transmission line resonator), an auxiliary superconducting three-level system [43, 44] with Δ -shaped transition is introduced to induce a controllable squeezed field in the cavity. Such a controllable quantum squeezed field can be further used to entangle two qubits in open environments. Optimally, one can obtain a maximum concurrence of about 0.31 and a maximum fidelity of about 0.65 for the above systems.

Even though the proposed strategy can be used to protect quantum entanglement, the obtained entanglement may not be high enough to be used in quantum information processing. Additional entanglement purification processes (e.g., [33]) should be introduced to increase the stationary entanglement. These procedures could make the superconducting circuit too complex. For this reason, further research (possibly using the methods in Ref. [46]) will be focused on modifying our proposal to obtain higher stationary entanglement.

Another interesting problem would be to develop a short-time regime entanglement-protection strategy, e.g., to protect entanglement during the gate operation process. In this regime, the correlation effects of the environmental noises should be considered, which leads to non-Markovian noises [47]. Different effects may be produced under non-Markovian noises. The existing decoherence suppression strategies [48, 49] against non-Markovian noises may be helpful to solve this problem.

ACKNOWLEDGMENTS

FN acknowledges partial support from the National Security Agency (NSA), Laboratory Physical Science (LPS), Army Research Office (ARO), National Science Foundation (NSF) grant No. EIA-0130383, JSPS-RFBR 06-02-91200. J. Zhang was supported by the National Natural Science Foundation of China under Grant Nos. 60704017, 60433050, 60635040, 60674039 and China Postdoctoral Science Foundation. T. J. Tarn would also like to acknowledge partial support from the U.S. Army Research Office under Grant W911NF-04-1-0386.

APPENDIX A: DERIVATION OF THE MAXIMUM CONCURRENCE AND FIDELITY

In this appendix, we show the derivation of the concurrence C of the stationary state ρ_∞ and the fidelity F between ρ_∞ and the maximally-entangled state ρ_m . Thus, we will derive Eq. (6) in the main text.

In order to simplify our discussions, let us use the so-called coherent vector picture as in Refs. [50, 51]. Considering the inner product $\langle X, Y \rangle = \text{tr}(X^\dagger Y)$, we can find the following matrix basis for all two-qubit matrices:

$$\left\{ \frac{1}{2}I_{4 \times 4}, \Omega_{14}^x, \Omega_{14}^y, \Omega_{23}^x, \Omega_{23}^y, \frac{1}{2}\sigma_x^{(1)}, \frac{1}{2}\sigma_y^{(1)}, \frac{1}{2}\sigma_x^{(2)}, \frac{1}{2}\sigma_y^{(2)}, \frac{1}{2}\sigma_x^{(1)}\sigma_z^{(2)}, \frac{1}{2}\sigma_z^{(1)}\sigma_x^{(2)}, \frac{1}{2}\sigma_y^{(1)}\sigma_z^{(2)}, \frac{1}{2}\sigma_z^{(1)}\sigma_y^{(2)}, \Omega_{14}^z, \Omega_{23}^z, \frac{1}{2}\sigma_z^{(1)}\sigma_z^{(2)} \right\}, \quad (\text{A1})$$

where $I_{4 \times 4}$ is the 4×4 identity matrix, and $\Omega_{14}^x, \Omega_{14}^y, \Omega_{23}^x, \Omega_{23}^y, \Omega_{14}^z, \Omega_{23}^z$ are defined as:

$$\begin{aligned} \Omega_{14}^x &= \begin{pmatrix} & & \frac{1}{\sqrt{2}} \\ & 0 & \\ \frac{1}{\sqrt{2}} & & \end{pmatrix}, \quad \Omega_{14}^y = \begin{pmatrix} & & \frac{-i}{\sqrt{2}} \\ & 0 & \\ \frac{i}{\sqrt{2}} & & \end{pmatrix}, \\ \Omega_{23}^x &= \begin{pmatrix} & & 0 \\ \frac{1}{\sqrt{2}} & & \\ 0 & \frac{1}{\sqrt{2}} & \end{pmatrix}, \quad \Omega_{23}^y = \begin{pmatrix} & & 0 \\ \frac{-i}{\sqrt{2}} & & \\ 0 & \frac{i}{\sqrt{2}} & \end{pmatrix}, \\ \Omega_{14}^z &= \begin{pmatrix} \frac{1}{\sqrt{2}} & & \\ & 0 & \\ & & \frac{-1}{\sqrt{2}} \end{pmatrix}, \quad \Omega_{23}^z = \begin{pmatrix} 0 & & \\ \frac{1}{\sqrt{2}} & & \\ & \frac{-1}{\sqrt{2}} & 0 \end{pmatrix}. \end{aligned}$$

The system density matrix ρ can be expanded under this matrix basis as:

$$\rho = \frac{1}{4}I_{4 \times 4} + \sum_{i=1}^{15} m_i \Omega_i,$$

where Ω_i ($i = 1, \dots, 15$) are all traceless basis matrices in (A1) and $m_i = \text{tr}(\Omega_i \rho)$.

Let $m = (m_1, \dots, m_{15})^T$, and thus the master equation (2) can be rewritten as [50, 51]:

$$\dot{m} = O_A m + D m + g, \quad (\text{A2})$$

where O_A is the adjoint representation matrix of $-iH_A$ and $(Dm + g)$ is the coherent vector representation of the Lindblad terms:

$$\sum_{j=1}^2 \Gamma_1 \mathcal{D}[\sigma_{-j}] \rho + \sum_{j=1}^2 2\Gamma_\phi [\sigma_{zj}] \rho,$$

with $D \leq 0$ and g a constant vector. Further, let

$$\begin{aligned} m^p &= (m_{14}^x, m_{14}^y, m_{23}^x, m_{23}^y)^T, \\ m^n &= (m_{14}^z, m_{23}^z, m_{zz})^T, \\ m^\epsilon &= (m_{x0}, m_{y0}, m_{0x}, m_{0y}, m_{xz}, m_{zx}, m_{yz}, m_{zy})^T, \end{aligned}$$

where

$$\begin{aligned} m_{14}^\alpha &= \text{tr}(\Omega_{14}^\alpha \rho), \quad m_{23}^\beta = \text{tr}(\Omega_{23}^\beta \rho), \quad \alpha, \beta = x, y, z, \\ m_{\alpha\beta} &= \text{tr} \left[\left(\frac{1}{2} \sigma_\alpha^{(1)} \sigma_\beta^{(2)} \right) \rho \right], \quad \alpha, \beta = 0, x, y, z, \end{aligned}$$

and $\sigma_0^{(j)} = I_{2 \times 2}$ ($j = 1, 2$) are 2×2 identity matrices acting on the qubit j . Then, we can rewrite Eq. (A2) as:

$$\begin{aligned} \dot{m}^p &= O_0^p m^p + \sum_{i=1}^4 u_i O_i^\eta m^\eta + D^p m^p, \\ \dot{m}^n &= \sum_{i=1}^4 u_i (-O_i^T) m^p + D^n m^n + g^n, \quad (\text{A3}) \\ \dot{m}^\epsilon &= \sum_{i=1}^4 u_i O_i^\epsilon m^\epsilon + D^\epsilon m^\epsilon, \end{aligned}$$

where $D^p = -4(\Gamma_1 + 2\Gamma_\phi)I_{4 \times 4} = -8\Gamma_2 I_{4 \times 4}$ and

$$\begin{aligned} u_1 &= 8\mu_1 \cos \theta_1, \quad u_2 = 8\mu_1 \sin \theta_1, \\ u_3 &= 8\mu_2 \cos \theta_2, \quad u_4 = -8\mu_2 \sin \theta_2, \end{aligned}$$

$$O_0^p = \begin{pmatrix} 0 & \Omega \\ -\Omega & 0 \\ & & 0 & \omega_{a1} - \omega_{a2} \\ & & \omega_{a2} - \omega_{a1} & 0 \end{pmatrix},$$

$$O_1^\eta = \begin{pmatrix} 0 & 0 & 0 \\ -1 & 0 & 0 \\ 0 & 0 & 0 \\ 0 & 0 & 0 \end{pmatrix}, \quad O_2^\eta = \begin{pmatrix} 1 & 0 & 0 \\ 0 & 0 & 0 \\ 0 & 0 & 0 \\ 0 & 0 & 0 \end{pmatrix},$$

$$O_3^\eta = \begin{pmatrix} 0 & 0 & 0 \\ 0 & 0 & 0 \\ 0 & 0 & 0 \\ 0 & -1 & 0 \end{pmatrix}, \quad O_4^\eta = \begin{pmatrix} 0 & 0 & 0 \\ 0 & 0 & 0 \\ 0 & 1 & 0 \\ 0 & 0 & 0 \end{pmatrix},$$

$$D^\eta = \begin{pmatrix} -4\Gamma_1 & 0 & 0 \\ 0 & -4\Gamma_1 & 0 \\ 4\sqrt{2}\Gamma_1 & 0 & -8\Gamma_1 \end{pmatrix}, \quad g^\eta = \begin{pmatrix} 2\sqrt{2}\Gamma_1 \\ 0 \\ 0 \end{pmatrix}. \quad (\text{A4})$$

D^ϵ and O_i^ϵ in the last equation in Eq. (A3) are respectively negative and traceless skew-symmetric matrices.

With simple calculations, we can obtain the following stationary solution of Eq. (A3):

$$\begin{aligned} m^\epsilon(\infty) &= 0, \quad m_{23}^x(\infty) = m_{23}^y(\infty) = m_{23}^z(\infty) = 0, \\ m_{14}^x(\infty) &= \frac{1}{\sqrt{2}}p \cos(\theta_1 - \phi), \quad m_{14}^y(\infty) = \frac{1}{\sqrt{2}}p \sin(\theta_1 - \phi), \\ m_{14}^z(\infty) &= \frac{\sqrt{2}}{4} \left\{ 1 + \sqrt{1 - \frac{8\Gamma_2}{\Gamma_1} p^2} \right\}, \\ m_{zz}(\infty) &= \frac{1}{4} \left\{ 1 + \sqrt{1 - \frac{8\Gamma_2}{\Gamma_1} p^2} \right\}, \end{aligned}$$

where p and ϕ are given in Eq. (5), from which we can

calculate the stationary state ρ_∞ and the stationary fidelity $F(\rho_\infty)$ in Eq. (6).

Further, recall that the concurrence of the quantum state

$$\rho = \begin{pmatrix} a & & w \\ & b & z \\ & z^* & c \\ w^* & & d \end{pmatrix}$$

can be analytically solved as [52]:

$$C(\rho) = 2 \max\{|w| - \sqrt{bc}, |z| - \sqrt{ad}, 0\},$$

from which we can obtain the stationary concurrence $C(\rho_\infty)$ in Eq. (6).

-
- [1] Y. Makhlin, G. Schön, and A. Shnirman, *Rev. Mod. Phys.* **73**, 357 (2001).
- [2] G. Wendin and V. S. Shumeiko, Superconducting quantum circuits, qubits, and computing, *Handbook of Theoretical and Computational Nanoscience* (Germany: Forschungszentrum Karlsruhe) and preprint arxiv: cond-mat/0508729.
- [3] J. Q. You and F. Nori, *Physics Today* **58** (11), 42 (2005).
- [4] J. Clarke, F. K. Wilhelm, *Nature* **453**, 1031 (2008).
- [5] Yu. A. Pashkin, T. Yamamoto, O. Astafiev, Y. Nakamura, D. Averin, and J. Tsai, *Nature* **421**, 823 (2003).
- [6] T. Yamamoto, Yu. A. Pashkin, O. Astafiev, Y. Nakamura, and J. Tsai, *Nature* **425**, 941 (2003).
- [7] A. J. Berkley, H. Xu, R. C. Ramos, M. A. Gubrud, F. W. Strauch, P. R. Johnson, J. R. Anderson, A. J. Dragt, C. J. Lobb, and F. C. Wellstood, *Science* **300**, 1548 (2003).
- [8] A. Izmalkov, M. Grajcar, E. Il'ichev, Th. Wagner, H. G. Meyer, A. Yu. Smirnov, M. H. S. Amin, A. Maassen van den Brink, and A. M. Zagoskin, *Phys. Rev. Lett.* **93**, 037003 (2004).
- [9] J. B. Majer, F. G. Paauw, A. C. J. terHaar, C.J.P.M. Harmans, and J. E. Mooij, *Phys. Rev. Lett.* **94**, 090501 (2005).
- [10] R. McDermott, R. W. Simmonds, M. Steffen, K. B. Cooper, K. Cicak, K. D. Osborn, S. Oh, D. P. Pappas, and J. M. Martinis, *Science* **307**, 1299 (2005).
- [11] T. Hime, P. A. Reichardt, B. L. T. Plourde, T. L. Robertson, C. E. Wu, A. V. Ustinov, and J. Clarke, *Science* **314**, 1427 (2006); I. Siddiqi and J. Clarke, *Science* **313**, 1400 (2006).
- [12] Y.-X. Liu, L. F. Wei, J. S. Tsai, and F. Nori, *Phys. Rev. Lett.* **96**, 067003 (2006); G. S. Paraoanu, *Phys. Rev. B* **74**, 140504(R) (2006).
- [13] J. Li, K. Chalapat, and G. S. Paraoanu, *Phys. Rev. B* **78**, 064503 (2008).
- [14] S. Ashhab, A. O. Niskanen, K. Harrabi, Y. Nakamura, T. Picot, P. C. de Groot, C.J.P.M. Harmans, J. E. Mooij, and F. Nori, *Phys. Rev. B* **77**, 014510 (2008); S. Ashhab and F. Nori, *Phys. Rev. B* **76**, 132513 (2007); S. Ashhab, S. Matsuo, N. Hatakenaka, and F. Nori, *Phys. Rev. B* **74**, 184504 (2006); C. Rigetti, A. Blais, and M. Devoret, *Phys. Rev. Lett.* **94**, 240502 (2005).
- [15] Y. Makhlin, G. Schön, and A. Shnirman, *Nature* **398**, 305 (1999).
- [16] Y.-X. Liu, C. P. Sun, and F. Nori, *Phys. Rev. A* **74**, 052321 (2006); C. M. Wilson, T. Duty, F. Persson, M. Sandberg, G. Johansson, and P. Delsing, *Phys. Rev. Lett.* **98**, 257003 (2007).
- [17] R. Migliore and A. Messina, *Phys. Rev. B* **72**, 214508 (2005).
- [18] S. H. W. van der Ploeg, A. Izmalkov, A. M. van den Brink, U. Hübner, M. Grajcar, E. Il'ichev, H. G. Meyer, and A. M. Zagoskin, *Phys. Rev. Lett.* **98**, 057004 (2007).
- [19] Y. D. Wang, P. Zhang, D. L. Zhou, and C. P. Sun, *Phys. Rev. B* **70**, 224515 (2004); L. F. Wei, Y.-X. Liu, and F. Nori, *Phys. Rev. B* **71**, 134506 (2005).
- [20] A. T. Sornborger, A. N. Cleland, and M. R. Geller, *Phys. Rev. A* **70**, 052315 (2004); M. R. Geller and A. N. Cleland, *Phys. Rev. A* **71**, 032311 (2005); E. J. Pritchett and M. R. Geller, *Phys. Rev. A* **72**, 010301(R) (2005); F. Xue, Y. D. Wang, C. P. Sun, H. Okamoto, H. Yamaguchi, *New J. Phys.* **9**, 35 (2007).
- [21] J. Q. You and F. Nori, *Phys. Rev. B* **68**, 064509 (2003); J. Q. You, J. S. Tsai, and F. Nori, *Phys. Rev. B* **68**, 024510 (2003); Y.-X. Liu, L. F. Wei, and F. Nori, *Europhys. Lett.* **67**, 941 (2004).
- [22] M. Wallquist, V. S. Shumeiko, and G. Wendin, *Phys. Rev. B* **74**, 224506 (2006); M. Paternostro, M. S. Tame, G. M. Palma, and M. S. Kim, *Phys. Rev. A* **74**, 052317 (2006).
- [23] A. Blais, J. Gambetta, A. Wallraff, D. I. Schuster, S. M. Girvin, M. H. Devoret, and R. J. Schoelkopf, *Phys. Rev. A* **75**, 032329 (2007).
- [24] Y.-X. Liu, L. F. Wei, J. R. Johansson, J. S. Tsai, and F. Nori, *Phys. Rev. B* **76**, 144518 (2007); M. Grajcar, Y.-X. Liu, F. Nori, and A. M. Zagoskin, *Phys. Rev. B* **74**, 172505 (2006); X.-L. He, Y.-X. Liu, J. Q. You,

- and F. Nori, Phys. Rev. A **76**, 022317 (2007); X.-L. He, J. Q. You, Y.-X. Liu, L. F. Wei, and F. Nori, Phys. Rev. B **76**, 024517 (2007).
- [25] L. F. Wei, Y.-X. Liu, and F. Nori, Phys. Rev. Lett. **96**, 246803 (2006); L. F. Wei, Y.-X. Liu, M. J. Storcz, and F. Nori, Phys. Rev. A **73**, 052307 (2006).
- [26] D. Braun, Phys. Rev. Lett. **89**, 277901 (2002); F. Benatti, R. Floreanini, and M. Piani, Phys. Rev. Lett. **91**, 070402 (2003).
- [27] S. Nicolosi, A. Napoli, A. Messina, and F. Petruccione, Phys. Rev. A **70**, 022511 (2004).
- [28] L. M. Duan and G. C. Guo, Phys. Rev. Lett. **79**, 1953 (1997); D. A. Lidar, I. L. Chuang, and K. B. Whaley, Phys. Rev. Lett. **81**, 2594 (1998); L.-A. Wu and D. A. Lidar, Phys. Rev. Lett. **88**, 207902 (2002).
- [29] A. R. R. Carvalho, F. Mintert, S. Palzer, and A. Buchleitner, Eur. Phys. J. D **41**, 425 (2007).
- [30] D. F. Walls and G. J. Milburn, *Quantum Optics* (Springer-Verlag, Berlin, 1994).
- [31] W. K. Wootters, Phys. Rev. Lett. **80**, 2245 (1998).
- [32] C. H. Bennett, G. Brassard, S. Popescu, B. Schumacher, J. A. Smolin, and W. K. Wootters, Phys. Rev. Lett. **76**, 722 (1996); W. Dür and H. J. Briegel, Rep. Prog. Phys. **70**, 1381 (2007).
- [33] K. Maruyama and F. Nori, Phys. Rev. A **78**, 022312 (2008); T. Tanamoto, K. Maruyama, Y.-X. Liu, X. Hu, and F. Nori, arXiv: quant-ph/0807.4788.
- [34] F. Gaitan, Phys. Rev. B **63**, 104511 (2001); V. Plerou and F. Gaitan, Phys. Rev. B **63**, 104512 (2001).
- [35] O. Astafiev, Yu. A. Pashkin, Y. Nakamura, T. Yamamoto, and J. S. Tsai, Phys. Rev. Lett. **93**, 267007 (2004).
- [36] P. Bertet, I. Chiorescu, G. Burkard, K. Semba, C.J.P.M. Harmans, D. P. DiVincenzo, and J. E. Mooij, Phys. Rev. Lett. **95**, 257002 (2005).
- [37] J. Q. You, J. S. Tsai, and F. Nori, Phys. Rev. Lett. **89**, 197902 (2002); T. Yamamoto, M. Watanabe, J. Q. You, Yu. A. Pashkin, O. Astafiev, Y. Nakamura, F. Nori, and J. S. Tsai, Phys. Rev. B **77**, 064505 (2008).
- [38] C. J. Villas-Boas, N. G. de Almeida, R. M. Serra, and M. H. Y. Moussa, Phys. Rev. A **68**, 061801(R) (2003); N. G. de Almeida, R. M. Serra, C. J. Villas-Boas, and M. H. Y. Moussa, Phys. Rev. A **69**, 035802 (2004).
- [39] X. Hu, F. Nori, Phys. Rev. Lett. **76**, 2294 (1996); **79**, 4605 (1997); Phys. Rev. B **53**, 2419 (1996); Physica B **263**, 16 (1999).
- [40] X. Hu and F. Nori, *Squeezed Quantum States in Josephson Junctions*, UM preprint (1996); X. Hu, Univ. of Michigan (UM) Thesis (1996); see also <http://www-personal.umich.edu/~nori/squeezed.html>.
- [41] M. J. Everitt, T. D. Clark, P. B. Stiffell, A. Vourdas, J. F. Ralph, R. J. Prance, and H. Prance, Phys. Rev. A **69**, 043804 (2004).
- [42] A. M. Zagoskin, E. Il'ichev, M. W. McCutcheon, J. Young, F. Nori, arxiv: cond-mat/0804.4186v1.
- [43] Y.-X. Liu, J. Q. You, L. F. Wei, C. P. Sun, and F. Nori, Phys. Rev. Lett. **95**, 087001 (2005); F. Deppe, M. Mariantoni, E. P. Menzel, A. Marx, S. Saito, K. Kakuyanagi, H. Tanaka, T. Meno, K. Semba, H. Takayanagi, E. Solano, R. Gross, arXiv: cond-mat/0805.3294v1, Nature Physics, in press (2008).
- [44] J. Q. You, Y.-X. Liu, C. P. Sun, and F. Nori, Phys. Rev. B **75**, 104516 (2007).
- [45] T. Lindstrom, C. H. Webster, J. E. Healey, M. S. Colclough, C. M. Muirhead, and A. Ya. Tzalenchuk, Supercond. Sci. Technol. **20**, 814 (2007).
- [46] M. Zhang, H. Y. Dai, Z. R. Xi, H. W. Xie, and D. W. Hu, Phys. Rev. A **76**, 042335 (2007).
- [47] W. T. Strunz, L. Diosi, and N. Gisin, Phys. Rev. Lett. **82**, 1801 (1999); T. Yu, Phys. Rev. A **69**, 062107 (2004).
- [48] G. Gordon, N. Erez, and G. Kurizki, J. Phys. B: At. Mol. Opt. Phys. **40**, S75 (2007); L. Viola and S. Lloyd, Phys. Rev. A **58**, 2733 (1998); G. Ithier, E. Collin, P. Joyez, P. J. Meeson, D. Vion, D. Esteve, F. Chiarello, A. Shnirman, Y. Makhlin, J. Schrieffer, and G. Schön, Phys. Rev. B **72**, 134519 (2005).
- [49] W. Cui, Z. R. Xi, and Y. Pan, Phys. Rev. A **77**, 032117 (2008).
- [50] R. Alicki and K. Lendi, *Quantum Dynamical Semigroup and Applications* (Springer-Verlag, New York, 1985).
- [51] C. Altafini, J. Math. Phys. **44**, 2357 (2003); J. Zhang, C. W. Li, R. B. Wu, T. J. Tarn, and X. S. Liu, J. Phys. A: Math. Gen. **38**, 6587 (2005); J. Zhang, R. B. Wu, C. W. Li, T. J. Tarn, and J. W. Wu, Phys. Rev. A **75**, 022324 (2007).
- [52] T. Yu, J. H. Eberly, Phys. Rev. Lett. **93**, 140404 (2004); T. Yu, J. H. Eberly, Phys. Rev. Lett. **97**, 140403 (2006).